Laboratory Investigation (2020) 100:630–642
https://doi.org/10.1038/s41374-019-0338-2

ARTICLE

Shp2-mediated MAPK pathway regulates ΔNp63 in epithelium to promote corneal innervation and homeostasis

Yuka Okada[1,2] · Yujin Zhang[1] · Lingling Zhang[1] · Lung-Kun Yeh[3] · Yen-Chiao Wang[1] · Shizuya Saika[2] · Chia-Yang Liu[1]

Received: 2 July 2019 / Revised: 19 August 2019 / Accepted: 30 August 2019 / Published online: 25 October 2019

Abstract

Corneal nerve fibers serving sensory, reflex, and neurotrophic functions sustain corneal homeostasis and transparency to promote normal visual function. It is not known whether corneal epithelium is also important for the corneal innervation. Herein, we generated a compound transgenic mouse strain, *K14rtTA;tetO-Cre* (*TC*);*Shp2*$^{flox/flox}$, in which *Shp2* was conditionally knocked out from K14-positive cells including corneal epithelium (*Shp2*$^{K14ce\text{-}cko}$) upon doxycycline (dox) administration. Our data reveal that *Shp2*$^{K14ce\text{-}cko}$ caused corneal denervation. More specifically, corneal epithelium thickness and corneal sensitivity reduced dramatically in *Shp2*$^{K14ce\text{-}cko}$ mice. In addition, corneal epithelial wound healing after debridement was delayed substantially in the mutant mice. These defects manifested in *Shp2*$^{K14ce\text{-}cko}$ mice resemble the symptoms of human neurotrophic keratopathy. Our in vitro study shows that neurite outgrowth of the mouse primary trigeminal ganglion cells (TGCs) was inhibited when as cocultured with mouse corneal epithelial cells (TKE2) transfected by *Shp2*-, *Mek1/2*-, or *ΔNp63*-targeted siRNA but not by *Akt1/2*-targeted siRNA. Furthermore, *ΔNp63* RNA interference downregulated *Ngf* expression in TKE2 cells. Cotransfection experiments reveal that Shp2 tightly monitored ΔNp63 protein levels in HEK293 and TKE2 cells. Taken together, our data suggest that the Shp2-mediated MAPK pathway regulated ΔNp63, which in turn positively regulated *Ngf* in epithelium to promote corneal innervation and epithelial homeostasis

Introduction

The vertebrate cornea is the dome-shaped transparent outer surface of the eye. It contains five anatomic layers, which are the epithelium, Bowman's layer, the stroma, Descemet's membrane, and the endothelium. As the outermost layer, corneal epithelium (CE) consists of nonkeratinized, stratified squamous epithelial cells, which are held together by tight junctions, to form an effective barrier against fluid loss and pathogen penetration [1]. In addition, the CE is one of the most sensitive structures in the body as it is densely innervated with corneal nerve fibers [2]. The majority of the corneal nerves are afferent sensory nociceptors, derived from the first (ophthalmic) division of the fifth cranial (CNV1 or trigeminal) nerve [3]. These nerve fibers project into peripheral corneal stroma from the corneoscleral limbus. After entering the cornea, the main stromal nerve bundle gives rise through branching to smaller stromal nerves to form a midstromal plexus and then subepithelial plexus, which supplies all layers of the CE [2, 4, 5]. The proper patterning of corneal innervation renders the cornea to respond quickly to irritation, touch and pain, thus protecting the cornea from the potential harmful external environment and injuries. Moreover, corneal nerves are involved in modulating blink reflexes and tear production that maintain corneal proper hydration [6, 7]. Therefore, corneal innervation is crucial for sustaining corneal homeostasis and biological functions [8, 9].

Supplementary information The online version of this article (https://doi.org/10.1038/s41374-019-0338-2) contains supplementary material, which is available to authorized users.

✉ Yuka Okada
yokada@wakayama-med.ac.jp

✉ Chia-Yang Liu
liuchia@iu.edu

[1] Indiana University School of Optometry, Bloomington, IN, USA

[2] Department of Ophthalmology, Wakayama Medical University, School of Medicine, Wakayama, Japan

[3] Department of Ophthalmology, Chang-Gung Memorial Hospital, Linko, Taiwan

It has been postulated that constant, direct interaction between CE cells and corneal nerves exists during corneal development and homeostasis [10, 11]. Several lines of in vitro evidence from coculture of trigeminal ganglion cells (TGCs) and CE cells indicate that these two cell types do support one another through the secretion of trophic factors [12–17]. Substance P is one of important trophic factors and may associate with other growth factors, such as epidermal growth factor (EGF), to promote migration and proliferation of corneal epithelial cells during corneal healing [13]. Likewise, interaction between corneal nerves and the CE cells itself is thought to be necessary for proper nociception and corneal protection [3]. It is known that neurotrophin-3 derived from cornea can promote the expression of transient receptor potential A1 ion channels in the corneal nerves, which enhances CNV1 innervation during embryonic corneal development [18]. Moreover, it has been proposed that CE cells function as surrogate Schwann cells for their sensory nerves during homeostasis and in response to injury [11]. Therefore, the close interaction and interdependent relationship properly maintained between the CE cells and corneal nerves are required to grant a healthy and functional cornea. Any disruption of this relationship or interaction would have deleterious effects on the anatomic integrity of the cornea, which may lead to persistent corneal disorders such as neurotrophic keratopathy (NK).

NK is a rare degenerative disease with reduction or absence of corneal sensation characterized by progressive damage to CE cells that can result in corneal perforation, with consequent loss of vision [19]. NK can be caused by a wide range of ocular and systemic diseases including congenital corneal anesthesia, dry eyes, and decreased eye blinking due to impaired corneal sensitivity, trauma, surgery, herpetic virus infection, misuse of topical medications, use of contact lenses, and even systemic conditions such as diabetes or vitamin A deficiency [20–22]. Currently, the diagnosis and treatment of NK are the most complex and challenging aspects of this disease, as the cellular and molecular pathogenesis of the NK syndrome remains elusive and a satisfactory therapeutic approach is not yet available [23]. Therefore, understanding the role of key signaling molecules which modulate the interplay between CE cells and trigeminal nerves will facilitate the development of novel treatments for this disease. Among these signaling molecules, Shp2 may participate in CE stratification and corneal nerve innervation [24]. Shp2 is a member of Src-homology 2 domain-containing protein tyrosine phosphatase family [25]. It is widely expressed in most tissues and plays a fundamental role in various cell signal transductions that control multiple important cellular events, such as proliferation, apoptosis, and migration [26–29]. As a major mediator of cellular signaling transductions, Shp2 is in a naturally autoinhibited condition and is activated once an extracellular ligand like EGF binds to the EGF receptor (EGFR). When Shp2 binds the phosphor-EGFR (active form), the scaffolding proteins, Grb2 and Gab1, are able to form a functional complex relaying signals to downstream components, leading to the initiation or/and regulation of the cellular processes like cell proliferation [30]. We previously reported that genetic ablation of *Shp2* in K14-positive epithelial cells disrupted corneal epithelial stratification during mouse development [24]. In the current study, we further investigate the role of Shp2 during corneal epithelial homeostasis and corneal nerve innervation. Our data show that *Shp2* ablation in K14-positive epithelial cells impaired corneal epithelial maintenance; delayed epithelial debridement wound healing and caused CE nerve denervation with loss/decrease of corneal sensation, resembling the symptoms of NK. We also establish the concept that Shp2 signals through MEK/ERK pathway in the epithelium is critical for the maintenance of corneal epithelial innervation and homeostasis.

Materials and methods mice

Compound transgenic mouse strains *K14rtTA;tetO-Cre;* $Shp2^{flox/flox}$ and *K14rtTA;tetO- Cre;* $Shp2^{flox/flox}$*;Thy1-YFP* were generated through the natural mating of single transgenic mouse lines *K14-rtTA* [31], *tetO-Cre* [32], *Thy1-YFP* [33], and $Shp2^{flox/flox}$ [34], respectively. *Shp2* ablation in the K14-positive cells was achieved by administering doxycycline (Dox) chow to *K14rtTA;tetO-Cre;* $Shp2^{flox/flox}$ transgenic mice in the dam for 14 days from postnatal day (P60) to P74. Mouse corneas ($n = 6$) were collected after dox-induction 4, 6, 10, and 14 days, respectively. Genetic knockout of *Shp2* was also performed in compound transgenic mice *K14rtTA;tetO-Cre;* $Shp2^{flox/flox}$*;Thy1-YFP* by Dox treatment from P23 to P33 and corneas ($n = 6$) were collected at P33. YFP-positive corneal nerve fiber images were taken by Zeiss Axio Zoom V16 stereomicroscope. All experiments involving mice were approved by the Animal Care and Use Committee of Indiana University and conducted in accordance with the Association for Research in Vision and Ophthalmology Statement for the Use of Animals in Ophthalmic and Vision Research.

Hematoxylin and Eosin (H&E) histological staining analysis

Enucleated mouse eyes were fixed overnight in 4% paraformaldehyde (PFA) diluted in 1× phosphate buffered saline (PBS), followed by dehydration in a series of ascending

alcohol (50, 75, 95, and 100%) and paraffin embedding. Deparaffinized sections (5 m) were stained with H&E reagent following protocol as previously described [24].

Functional assay of corneal sensitivity in mice

Corneal sensitivity of alive experimental mice was measured by the handheld esthesiometer (Cochet-Bonnet) (Luneau Ophthalmologia, France). Mouse eyes ($n = 6$) of Dox-treated *K14-rtTA;TC;Shp2*$^{WT/WT}$ (control) and *K14-rtTA;TC;Shp2*$^{flox/flox}$ (*Shp2*$^{K14ce\text{-}cko}$), respectively, were measured 3 times and the length of nylon filament that elicited eyelid blinking was recorded and converted into average threshold pressure (g/mm^2) according to the formula provided by manufacturer. The normal corneal sensitivity ranges from 0.4 to 0.7 g/mm^2 (or 60–45 mm nylon filament length) [35].

Corneal whole mount immunostaining

Mouse corneas were fixed overnight in 4% PFA diluted in 0.1 M phosphate-buffer. The fixed corneas were carefully cut into a clover leaf shape and incubated in 0.2% sodium borohydride in 1× PBS for 1 h at room temperature. After three washes with 1× PBS, the corneas were incubated in 2N HCl, 0.5% TritonX-100 in 1× PBS for 1 h at room temperature. After one wash with 0.1 M phosphate buffer (pH 7.4) and two washes with 1× PBS, the corneas were incubated in 1 micro gm/ml bovine serum albumin in 50% TD (0.5% DMSO, 0.5% TritonX-100®, and 2.5% Dextran 40 in PBS) for 15 min at room temperature. The corneal samples were probed with neuron-specific class III beta-tubulin (Tuj1) northernlight™ NL-557-conjugate antibody at 1:10 dilution (R&D Systems; Cat#: NL1195R) for 24 h at 4 °C. After twice washes with 50%TD and one wash with 1× PBS. The corneal samples were mounted and observed under EVOS FL Auto Cell Imaging System (Invitrogen-Thermo Fisher Scientific).

Transmission electron microscopy

Corneal samples were fixed in 0.1 M cacodylate buffer (pH7.4) containing 3% glutaraldehyde and 2% PFA for 2 h at 4 °C and then were preserved in 0.1 M cacodylate buffer (pH 7.4) containing 0.5% glutaraldehyde at 4 °C overnight. After refixation in 1% osmium tetraoxide (OsO4) for 1 h at 4 °C, corneal samples were washed in 0.1 M cacodylate buffer (pH 7.4) three times for 10 min each, and then dehydrated in a graded ethanol series and embedded in Epon 812 epoxy resin (Polysciences, Inc., Warrington, PA). Ultrathin 50-nm sections were stained with uranyl acetate and lead citrate and images were photographed with a Hitachi 7500 Transmission Electron Microscope (Hitachi, Tokyo, Japan) equipped with AMT Digital camera.

Coculture of primary trigeminal ganglia and siRNA transfected TKE2 cells

TKE2 cells (ECACC 11033107) were cultured in six-well plates with 2 ml Keratinocyte-serum free medium (KSFM, Gibco #17005-042). At 30–40% cell confluence, TKE2 cells were transfected with different siRNA (10 nM) using lipofectamine RNAiMAX (Invitrogen, Cat: #13778) following the manufactural protocol to knockdown gene expression of *Shp2*, *Mek1/2*, *Akt1/2, and ΔNp63*, respectively. TKE2 cells transfected with nontarget control siRNA were used as negative control. The siRNAs used in this study were listed in Supplementary Table 1.

Primary culture of TGCs was prepared according to a method previously described [36] with a minor modification: trigeminal ganglia from five C57BL/6 mice at P10 were dissected, washed with ice-cold DMEM/F12, and enzymatically digested with 0.1% collagenase (Type I, Sigma, #C0130)/DMEM/F12 for 30 min at 37 °C followed by treatment with 0.05% trypsin/EDTA-HBS (Invitrogen, #25300-054) for 40 min at 37 °C. The digested ganglia were washed once with DMEM/F12 supplemented with 10% fetal calf serum and triturated with fire polished glass pipettes. The cell suspension was centrifuged at 2000 rpm for 2 min. Cell pellets were resuspended and seeded in DMEM/F12 supplemented with 10% fetal calf serum in six-well plates (~2.0×10^5 cells/well). The next day, cells were treated with 3 micro gm/ml of mitomycin-C at 37 °C for 2 h, washed with PBS. Then siRNA treated-TKE2 cells were added (~4.0×10^4 cells/well) and cocultured in KSFM for another 3 days.

Measurement of neurites outgrowth

Under stereomicroscope, each coculture well of TGCs with different siRNA transfected TKE2 cells was randomly selected for taking photographs. The length of neurites from each coculture ($n = 90$) was measured by a COMCURVE-9Jr pen-type curvimeter (Koizumi Sokki Mfg. Co., Ltd). Data from experiments repeated 3–5 times repeated were analyzed by the Student's *t*-test.

Transfection of Shp2 and ΔNp63 plasmid DNAs in HEK293, HTCE, or TKE2 cells

HEK293 cells (ATCC® CRL-1573™) cultured in six-well plates with DMEM medium containing 10% fetal bovine serum were cotransfected with a various amounts of *CMV-Shp2WT* (Addgene, #8381) and *ΔNp63-Flag* (Addgene, #26979) at 70% confluence as indicated in Fig. 5a using

calcium phosphate transfection kit (Thermal-Fisher Cat: K278001) according to the manufactural protocol. Forty-eight hours posttransfection, total protein isolated from cell lysates was subjected to western blotting to detect the expression of Shp2 and ΔNp63. To test whether Shp2 regulates ΔNp63 protein stability, HEK293 cells seeded in six-well plates were cotransfected with 1 micro gm/well *CMV-Shp2WT* and 2 micro gm/well.

ΔNp63-Flag and treated with a different amount of MG132 (Sigma-Aldrich, Cat:1211877-36-9) as indicated in Fig. 5b. Forty-eight hours after transfection, protein level of Shp2 and ΔNp63 was examined by western blotting analysis.

Immunocytofluorescence staining

TKE2 cells, cultured in four-well chamber slides with KSFM medium were transfected with 0.5 micro gm *Shp2-EGFP* plasmid (Addgene, #12283) using lipofectmine 2000 reagent (Invitrogene, Cat:11668-030) via reverse-transfection procedure according to the manufactural protocol. Forty-eight hours posttransfection, TKE2 cells were transiently fixed in 4% paraffin, blocked with 3% bovine serum albumin in PBS containing 0.05% NP-40 for 1 h at room temperature, and then incubated overnight at 4 °C with primary antibodies diluted in the same buffer. After three washes in 1× PBS containing 0.1% Tween 20 (PBST), slides were incubated at room temperature for 1 h with Alexa Fluor 488- and/or Alexa Fluor 555-conjugated secondary antibodies (Life Technologies) and 1 µg/ml DAPI as a nuclear counterstain. Following incubation, the slides were washed with PBST and mounted with Mowiol (Sanofi-Aventis). Sections were examined and photographed using a Zeiss Axio Observer Z1 microscope equipped with an Axiocam Mrm camera or EVOS FL Auto Cell Imaging System (Invitrogen-Thermo Fisher Scientific). Primary antibodies, mouse monoclonal anti-Flag antibody (sigma, Cat: F3040) and rabbit anti-ΔNp63 (Abcam, Cat: Ab166857) were used to detect Shp2 and ΔNp63 expression, respectively. The secondary antibodies, goat anti-mouse IgG-Alex488 (Thermo-Fisher Scientific, A-11001), and goat anti-rabbit IgG-Alex555 (Thermo-Fisher Scientific, A27039) were used to assist in the detection by the immunostaining.

Healing of an epithelial defect in in vivo mouse cornea

Under general anesthesia, a round epithelial defect (2.0 mm in diameter) was produced in the central cornea of the right eye of a mouse as using a skin biopsy trephine and microsurgical blade in each experiment as previously reported [37, 38]. At specific intervals during the healing process, each cornea was processed for evaluation of the epithelial defect closure. Epithelial closure the cornea was evaluated by measuring the size of green fluorescein-stain of the defect of the epithelium as previously reported [39].

Real-time quantitative PCR (RT-qPCR) and reverse transcription PCR (RT-PCR)

Total RNA (10 micro gm) was isolated from TKE2 or HEK293 cells using Trizol reagent (Invitrogen), then annealed to random primers and reverse transcribed with avian reverse transcriptase (RT) kits (Promega), according to the manufacturer's instructions. RT-PCR was performed using C1000 Touch Thermal cycler (Bio-Rad Laboratories Inc.). 30-35 PCR cyclers were carried out to detect the expression of Bmp4 and housekeeping gene *Gapdh*. RT-qPCR was performed using the CFX96 real-time system equipped with a C1000™ Thermal Cycler (Bio-Rad Laboratories Inc.). After the initial 3 min denaturing step at 95 °C, 40 subsequent cycles at 95 °C lasting 15 s, 62 °C for 15 s, and 72 °C for 20 s were performed. The cycle threshold values were used to calculate the normalized expression of genes of interest against *Gapdh* using Q-Gene software. RT-qPCR primer *Shp2*-F 5′ GTCCACCACA AGCAGGAGAG and *Shp2*-R GAACGTCGATGTCAC AGTCC was used for *Shp2* expression in TKE2 cells.

Primer *ΔNp63*-F 5′ GGAAAACAATGCCCAGACT CAA and *ΔNp63*-R 5′GGTCACTGAGGTCTGAGTCT was used to examine *ΔNp63* expression in TKE2 cells.

Primer m*Ngf* F 5′ CTGTGCCTCAAGCCAGTGAA and m*Ngf* R 5′ TCACTGCGGCCAGTATAGAA was used to examine Ngf expression in TKE2 cells.

Primer *Gapdh*-F 5′ AGGTGGTGAAGCAGGCATCT and *Gapdh*-R 5′ TTACTCCTTGGAGGCCATGT was used to detect *Gapdh* expression in TKE2 cells.

Western blotting analysis

TKE2 or HEK293 cells were homogenized in RIPA buffer (50 mM Tris base, 150 mM NaCl, 0.5% deoxycholic acid-sodium salt, 2% SDS, and 1% NP40, pH 7.5) containing 1× protease inhibitor cocktail (Sigma P8340). Cell lysates (20 micro gm) from each sample were separated on a 4–20% linear gradient Tris-HCl denaturing polyacrylamide Ready Gel (Bio-Rad) and transferred to PVDF membrane (Whatman). Membranes were blocked with 5% nonfat milk in TBST (10 mM Tris-HCl pH 8.0, 150 mM NaCl, and 0.05% Tween 20) and probed with primary antibody in the same buffer overnight at 4 °C. After three washes in TBST, membranes were probed with HRP-conjugated secondary antibody for an hour at room temperature and bond second antibody was further detected using an enhanced chemiluminescence assay (Supersignal West Pico, #34080; Thermo-Fisher Scientific) and examined and photographed

using a VersaDoc 4000MP imaging system (Bio-Rad). Primary antibodies, rabbit anti-Shp2 (D50F2) (cell signaling, Cat: 3397 P), rabbit anti-ΔNp63 (Abcam, ab166857), rabbit anti-Ngf (LSBio LS-C171793), and goat anti-beta-actin (Santa Cruz, sc-1616) were used to examine expression of Shp2, ΔNp63, Ngf, and beta-actin, respectively. The secondary antibodies, goat anti-rabbit IgG-HRP (Thermo-Fisher Scientific, G-21234), donkey anti-goat IgG-HRP (Thermo-Fisher Scientific, A16005) were used to assist in the detection by western blots.

Statistical analysis

A two-tailed Student's *t*-test (Excel, Microsoft, Redmond, WA, USA) was used to analyze the significance of difference; $*P < 0.05$ was considered statistically significant and $**P < 0.01$ was considered highly statistically significant.

Results

Corneal epithelial thinning and reduction of nociception in *Shp2*$^{K14ce\text{-}cko}$ adult mice

To explore the role of Shp2 in corneal epithelial homeostasis, Dox chow was administered in the dam to *K14-rtTA*;*TC*;*Shp2*$^{WT/WT}$ (control) and *K14-rtTA*;*TC*;*Shp2*$^{flox/flox}$ (*Shp2*$^{K14ce\text{-}cko}$) adult mice (Fig. 1a) from P60 for different periods of time as mentioned in "Materials and Methods". Histologic analysis by H&E stain clearly shows that the CE cells maintained 6–7 cell layers in control mice (Fig. 1b, d, f, h). In contrast, except for those with 4 days Dox treatment (Fig. 1c), the CE cells were dramatically reduced to 2–3 layers in *Shp2*$^{K14ce\text{-}cko}$ mice after Dox treatment (Fig. 1 e, g, i). These suggest that CE homeostasis was disrupted in *Shp2*$^{K14ce\text{-}cko}$ mice. In addition, deletion of *Shp2* in basal CE cells of *Shp2*$^{K14ce\text{-}cko}$ mice caused a progressive loss of corneal sensation starting from 10 days of Dox administration as examined by Cochet–Bonnet aesthesiometer (Fig. 1j). We found that the anatomical changes of CE in *Shp2*$^{K14ce\text{-}cko}$ mice were noticed at day 6 and then the reduction of corneal sensation occurred on day 10 after Dox treatment (Fig. 1e, j). This result demonstrates that disruption of CE in *Shp2*$^{K14ce\text{-}cko}$ mice significantly affected normal corneal sensation and corneal homeostasis.

Shp2 deficiency results in corneal denervation in *Shp2*$^{K14ce\text{-}cko}$ adult mice

The reduction of corneal sensation after *Shp2* ablation implied that corneal innervation might be impaired in *Shp2*$^{K14ce\text{-}cko}$ mice. To address this concern, corneal

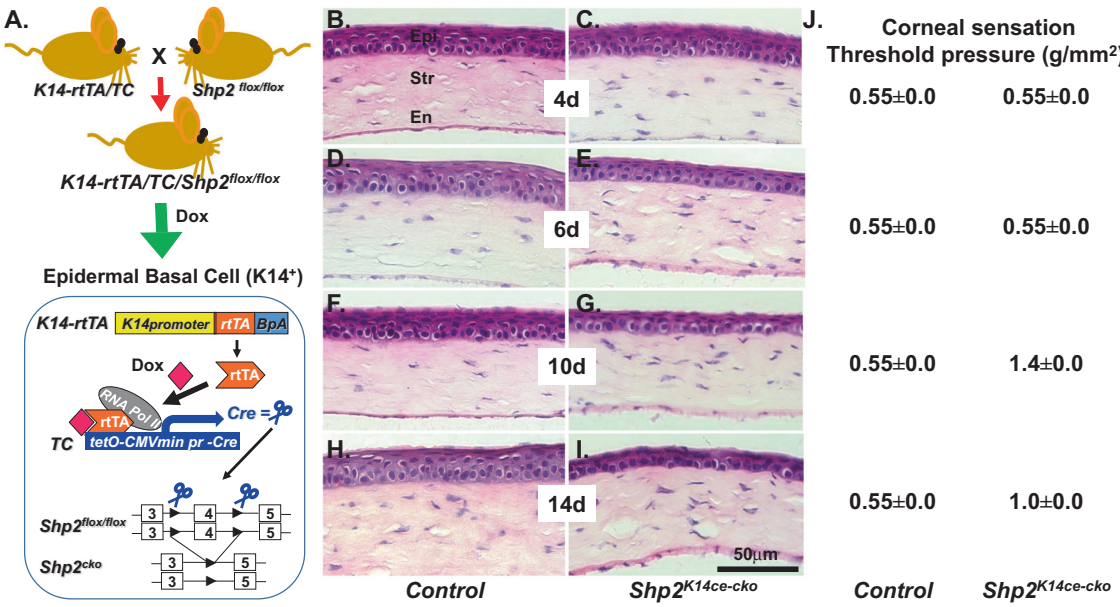

Fig. 1 *Shp2* is essential for corneal epithelial homeostasis. **a** Schematic representation of Dox-inducible ablation of Shp2 gene specifically in K14 expressing cells including the corneal basal cells of the triple transgenic mice (*K14-rtTA*;*TC*;*Shp2*$^{flox/flox}$). **b–i** H&E staining shows that the corneal epithelial thickness of the triple transgenic mice (**c**, **e**, **g**, **i**) was gradually reduced after Dox induction for 4, 6, 10, and 14 days, respectively, since P60 compared with litter controls (**b**, **d**, **f**, **h**). Note that the central corneal epithelial cell layers did not changed dramatically after 4 days of Dox induction (**c**). Cell layers significantly deduced since 6 days Dox induction (**e**). In contrast, control mice kept 6–7 stratified corneal epithelial cell layers after Dox induction. **j** Functional assay of corneal sensation were measured in three mice (six eyes) of each time point by Cochet–Bonnet aesthesiometer. Corneal sensitivity significantly reduced from 0.55 ± 0.0 to 1.4 ± 0.0 and 1.0 ± 0.0 (g/mm^2) at 10 and 14 days, respectively, after Dox administration. ($n = 6$, $P < 0.01$). Epi corneal epithelium, Str stroma, En endothelium

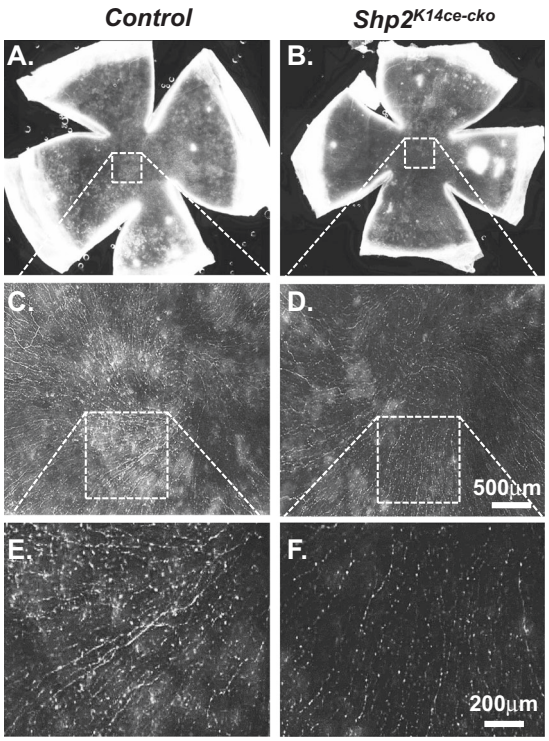

Fig. 2 *Shp2* deletion in corneal basal epithelial cells reduced nerve innervation density in corneal epithelium. **a**, **b** Representative whole mount overviews of mouse corneal epithelial nerve innervation from adult mice administered Dox for 10 days. **c–f** Detail structure of central corneal nerve networks. Note that *Shp2* deficiency resulted in lower density of corneal epithelial nerve fibers/bundles (compare **d** to **c**; **f** to **e**). In addition. Three mice ($n = 6$ corneas) of each group were examined. *Shp2* deficiency caused less nerve fibers in corneal epithelial nerve networks (compare **f** to **e**)

innervation was examined by whole-mount corneal immunofluorescent staining of Tuj1, a marker for sensory nerve fibers. Our data clearly show that the density of corneal nerve fibers was dramatically reduced in $Shp2^{K14ce\text{-}cko}$ as compared with littermate controls with 10 days' dox administration (Compare Fig. 2d, f with 2c, e). This result suggests that Shp2 in basal corneal epithelial cells of adult mice played critical role in the maintenance of corneal innervation.

Next, we took a closer look regarding the ultrastructure of corneal innervation by the transmission electron microscopy (TEM) in adult mice (Fig. 3). Control CE exhibited healthy nerve bundles in the epithelial basal layer (Fig. 3a, a′) and nerve fibers in subrabasal layers (Fig. 3c, c′). On the contrary, $Shp2^{K14ce\text{-}cko}$ mutant mice displayed degeneration in both nerve bundles and fibers (Fig. 3b, b′, d, d′).

In another set of experiments, we generated the quadruple transgenic mouse strain, *K14rtTA*;*TC*;$Shp2^{flox/flox}$;*Thy1-YFP*, in which yellow fluorescent protein (YFP) driven by Thy1 promoter is strongly expressed in motor and sensory neurons. We administered this strain and *Thy1-YFP* control mice with Dox chow from P23 to P33 to examine the possible damage in corneal innervation after *Shp2* ablation. YFP fluorescent images clearly demonstrate that Thy-1-positive corneal nerve networks were detected in control corneas as judged by nerve fibers/branches and nerve ending properly organized in the suprabasal layers, basal layer, epithelial–stromal junctions, and anterior and posterior stromal layers. In contrast, the Thy-1-YFP signal either was fragmented or absent in $Shp2^{K14ce\text{-}cko}$ mice (Figs. 4 and 5). Compared with what we observed in adult mice, these data suggest that more severe damage in corneal innervation after *Shp2* ablation occurred in young mice than those in elder ones. Taken together, these observations indicate that *Shp2* deficiency in basal corneal epithelial cells resulted in corneal denervation. This is consistent with loss/decrease of corneal sensation in the $Shp2^{K14ce\text{-}cko}$ mice.

Knockdown of MEK1/2 expression decreases neurite outgrowth of trigeminal ganglia in vitro

It is known that Shp2 transmits signals mainly through Mek and/or Akt in various cell types [40]. To define Shp2 downstream signaling pathway in CE cells for corneal innervation, we measured neurite outgrowth of mouse primary trigeminal ganglia cocultured with different siRNA transfected-TKE2 cells, in which *Shp2*, *Mek1/2*, or *Akt1/2* was knocked down with specific siRNA transfection, respectively. As shown in Fig. 6, TKE2 transfected with either *Shp2* siRNA or *Mek1/2* siRNA remarkably decreased the length of neurite of the primary cultured trigeminal ganglia as compared with control siRNA transfected-TKE2. However, TKE2 transfected with *Akt1/2* siRNA had no significance on the length of neurite from TGCs. These data suggest that Shp2 might transmit through MEK/ERK, but not PI3K/AKT downstream signaling to affect the behavior of corneal epithelial cells and corneal innervation.

Knockdown of *ΔNp63* affected Ngf expression in TKE2 cells and neuron outgrowth of trigeminal ganglia in vitro

To explore the downstream target of Shp2–MEK–ERK signaling transduction in CE, which may associate with corneal innervation, the transcription factor, ΔNp63 was selected to test this possibility since we previously found that ΔNp63 expression was dramatically reduced in $Shp2^{K14ce\text{-}cko}$ mice [24]. Indeed, qRT-PCR shows that *ΔNp63* mRNA level was downregulated to ~40% in *Shp2* siRNA-treated TKE2 cells (Fig.7a). Western blot analysis confirmed ΔNp63 protein level was also decreased in *Shp2* siRNA treated-TKE2 cells (Fig. 7b). In addition, coculture

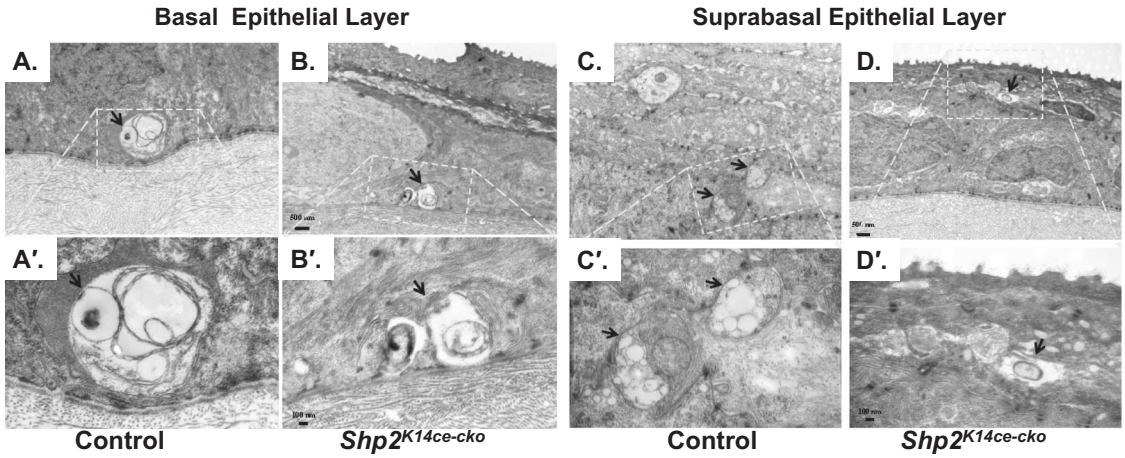

Fig. 3 Ablation of Shp2 in CE impaired corneal nerve bundle/fiber formation. Transmission electronic micrographs of control group (**a**, **a′**, **c**, **c′**) and *Shp2*^{K14cecko} (**b**, **b′**, **d**, **d′**). Control corneal epithelium exhibited healthy nerve bundles (arrow) in the epithelial basal layer (**a**, **a′**) and nerve fibers (arrows) in subrabasal layers (**c**, **c′**). In contrast, *Shp2*$^{K14ce-cko}$ displayed degeneration in both nerve bundles and fibers (**b**, **b′**, **d**, **d′**)

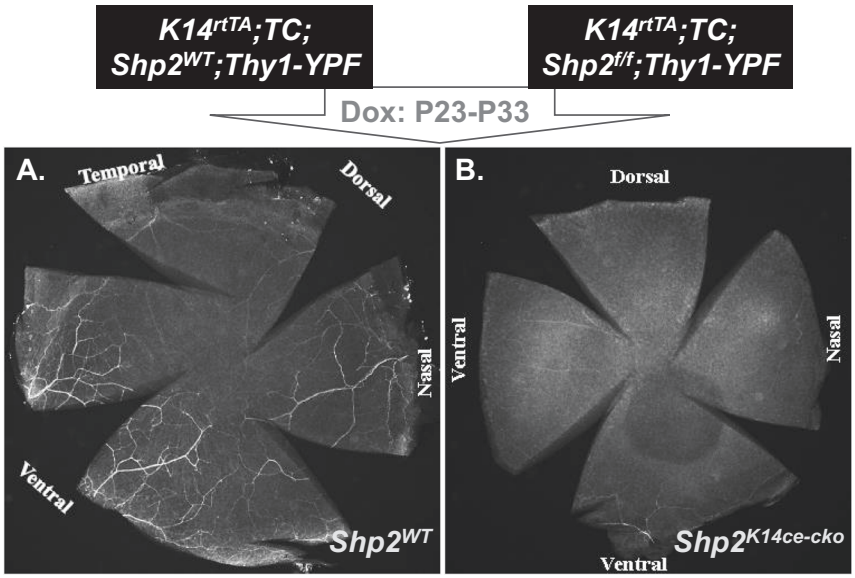

Fig. 4 Shp2 ablation resulted in corneal denervation. Whole-mount cornea YFP fluorescent images shows that nerve fibers were detected in *Shp2*^{WT} (**a**), while YFP was fragmented or absent in *Shp2*$^{K14ce-cko}$ (**b**)

experiments reveal that as compared with the control siRNA (Fig. 7c), either *Shp2* siRNA (Fig. 7d) or *ΔNp63* siRNA transfected-TKE2 cells (Fig. 7e) significantly reduced the length of neurite outgrowth of primary TGCs (Fig. 7f).

These data indicate that part of the interaction between TKE2 cells and TGCs through Shp2 might be through diffusible factors. Interestingly, indeed, Ngf protein expression level was downregulated in ΔNp63 siRNA (20 and 50 nM) transfected TKE2 cells (Fig. 8a, lanes 3 and 4). Likewise, *Ngf* mRNA level was also reduced ~90% in *Shp2*$^{K14ce-cko}$ mice as compared with that in *Shp2*^{WT} littermate (Fig. 8b). Taken together, our data suggest that Shp2 → MEK → ΔNp63 signaling axis at least in part positively regulated Ngf in CE, which was important for the maintenance of corneal epithelial innervation.

Shp2 tightly monitors ΔNp63 expression in cultured cells

To understand the mechanism by which Shp2 → MEK signaling regulated ΔNp63 expression in CE, HEK293 cells were cotransfected with CMV-*Shp2* cDNA and *CMV-ΔNp63* cDNA plasmids at different ratio for 48 h. Western blot analysis reveals that Shp2 controlled ΔNp63 protein levels in a dosage dependent manner (Fig. 9). As shown in lane 2 and lane 3 of Fig. 8a, cotransfection of HEK293 cells with ΔNp63 plasmid DNA (2 μg) and *Shp2* plasmid DNA (ranging from 0.01 to 0.1 μg), ΔNp63 protein expression levels were upregulated. However, *Shp2* plasmid concentration >1 μg caused downregulation of ΔNp63 protein (Fig. 9a, lanes 4–6). However, MG132,

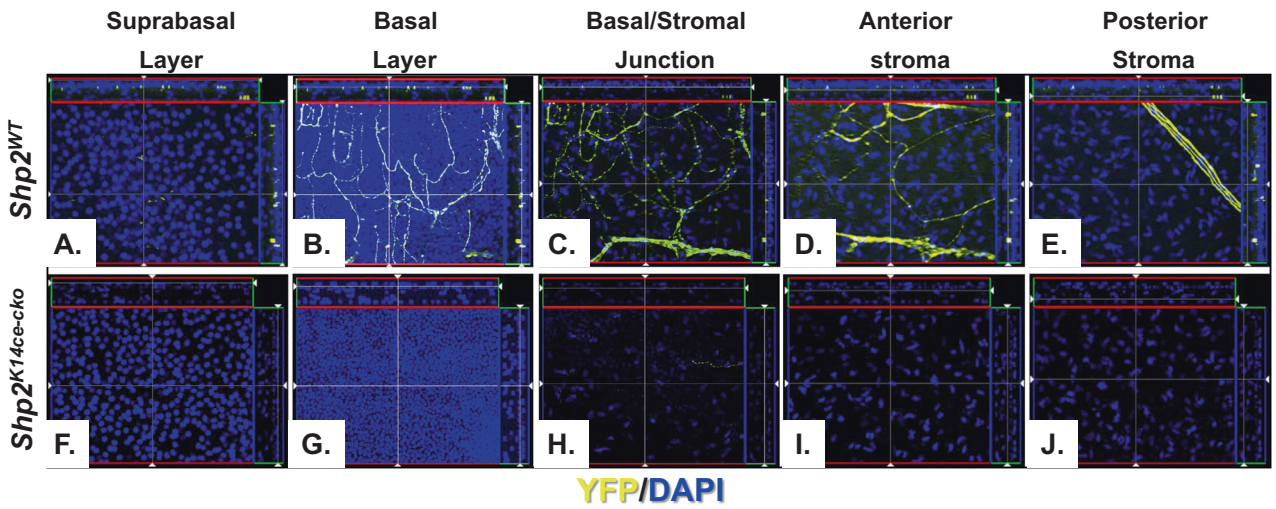

Fig. 5 Shp2 ablation caused corneal denervation. Images of YFP-positive optical sections were taken by ZEISS Apotome 2 from the central cornea of $Shp2^{WT}$ (**a–e**) and $Shp2^{K14ce\text{-}cko}$ (**f–j**) mice. Note that nerve fiber branches and endings were present in the suprabasal layer, basal layer, epithelial/stromal junction, and anterior and posterior stroma layer. In contrast, YFP signal was only fragmented or absent in $Shp2^{K14ce\text{-}cko}$

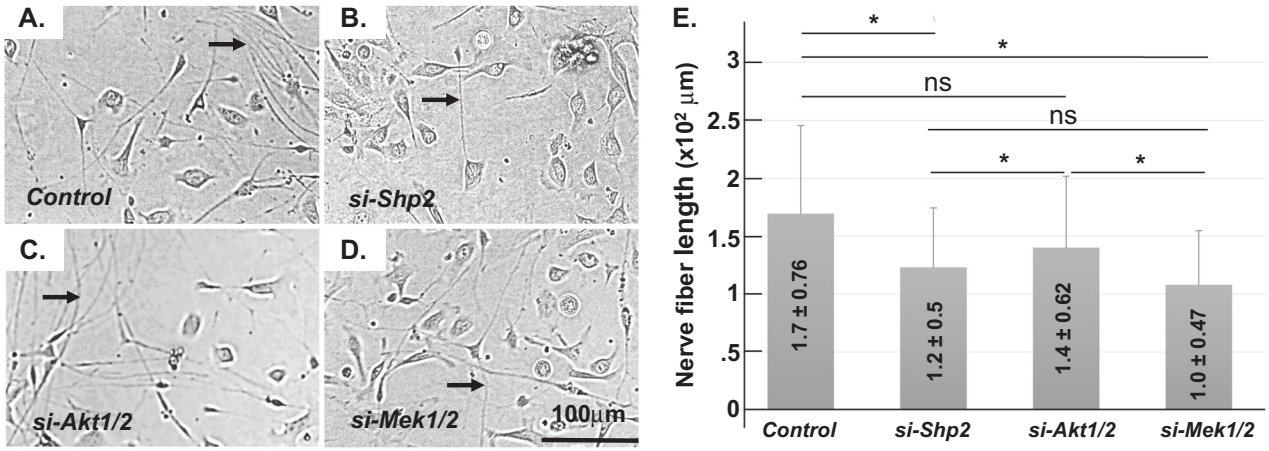

Fig. 6 Measurement of neurite outgrowth of mouse primary TGC co-cultured with siRNA-transfected TKE2 cells. Micrographs shows that TKE2 transfected with *Shp2* siRNA (**b**) or *Mek1/2* siRNA (**d**) impeded TGC neurite outgrowth as compared with control siRNA-transfected TKE2 (**a**). However, TKE2 transfected with *Akt1/2* siRNA (**c**) had no significant change on the neurite outgrowth (compare **c** with **a**). Arrows indicate neurite fibers (**a–d**). Histogram presentation of images of **a–d** (**e**). Three independent experiments have been performed. *($n = 90$, $P < 0.05$); NS no significance

a proteasome inhibitor, attenuated the inhibitory effect of high dosage Shp2 to ΔNp63 protein (Fig. 9b). More interestingly, cotransfection of the human corneal epithelial cell line (HTCE) with *CMV-Shp2* cDNA and *CMV-ΔNp63* cDNA plasmids indicate that Shp2 protein (red) and ΔNp63 protein (green) were exclusively presented in HTCE cells as shown by immunocytofluorescent staining (Fig. 9c). These data suggest that at normal/physiological condition, ΔNp63 protein level was positively regulated by Shp2. However, overexpression of Shp2 caused degradation of ΔNp63 protein. Taken together, our data suggest that ΔNp63 was tightly regulated by Shp2 in mouse corneal epithelial cells.

Shp2 deficiency delays corneal debridement wound healing in $Shp2^{K14ce\text{-}cko}$ adult mice

Our data demonstrate that Shp2 ablation impaired corneal epithelial homeostasis and sensation in $Shp2^{K14ce\text{-}cko}$ adult mice. These defects might affect corneal debridement wound healing. To test this hypothesis, we performed a 2.0 mm diameter corneal epithelial debridement and the

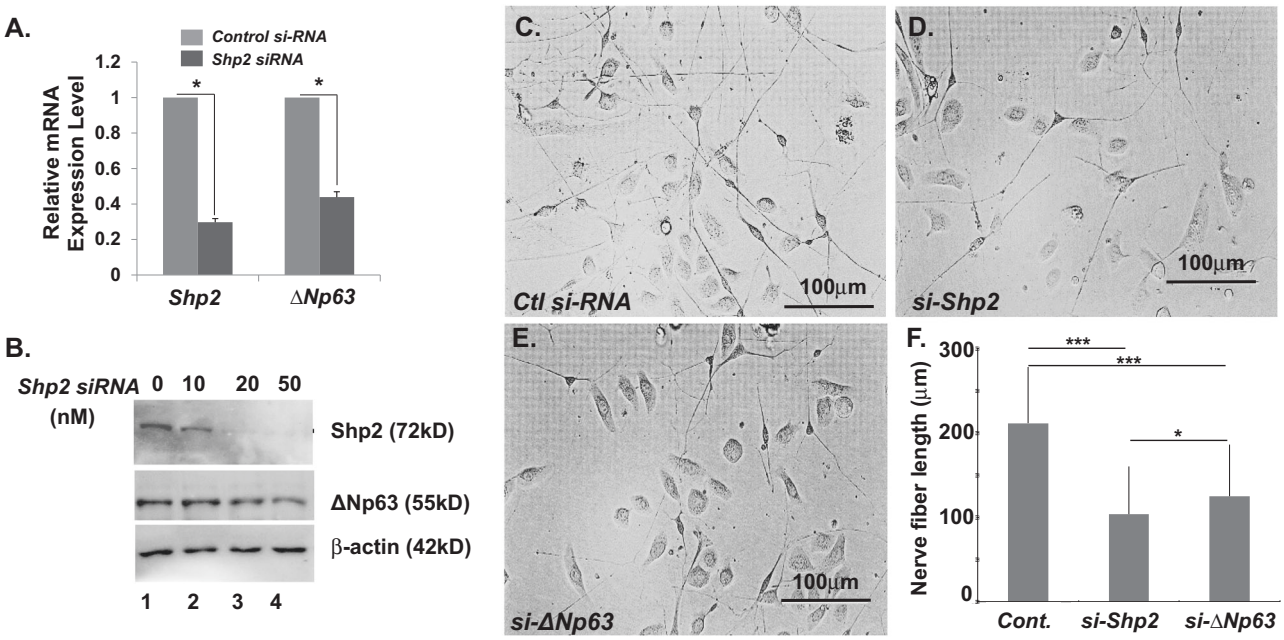

Fig. 7 Either *Shp2* or *ΔNp63* knockdown in TKE2 cells by siRNA transfection impeded neurite outgrowth of cocultured primary TGCs. **a** RT-qPCR analysis of *Shp2* and *ΔNp63* mRNA in TKE2 cells treated with control (*Ctl*) or *Shp2* siRNA (10 nM) for 48 h. $*n = 4$, $p < 0.05$. **b** Western blotting analysis of Shp2, ΔNp63, and β-actin in TKE2 cells transfected with 0, 10, 20, and 50 nM of *Shp2* siRNA for 48 h, respectively. **c–e** Micrographs shows that TKE2 transfected with *Shp2* siRNA (*si-Shp2*, **d**) or *ΔNp63* siRNA (*si-ΔNp63*, **e**) impeded neurite outgrowth as compared with control siRNA-transfected TKE2. **f** Histogram shows TGCs nerve fiber length from three independent experiments. All data are shown as mean ± SD. $*(n = 90, P < 0.05)$ $***(n = 90, p < 0.005)$

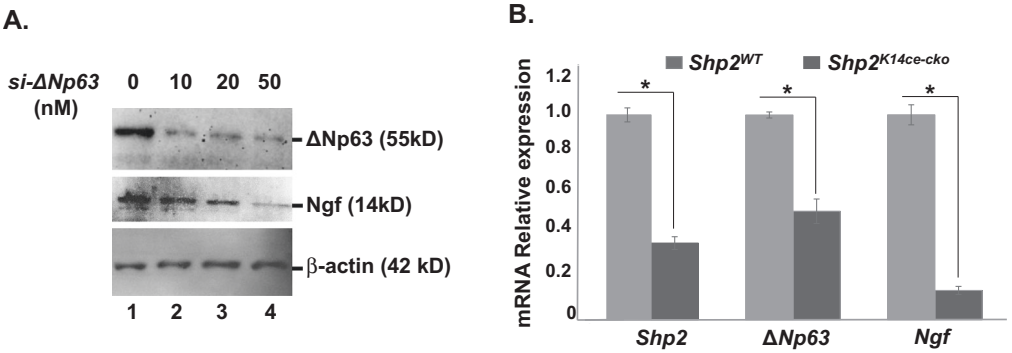

Fig. 8 Down regulation of Ngf in *ΔNp63* siRNA-transfected TKE2 cells and in $Shp2^{K14ce\text{-}cko}$ cornea. **a** Western blotting analysis shows that Ngf protein expression level was decreased in *si-ΔNp63* transfected TKE2 cells. **b** qRT-PCR analysis of *Shp2*, *ΔNp63*, and *Ngf* mRNAs in $Shp2^{WT}$ and $Shp2^{K14ce\text{-}cko}$ corneas. Note that the 35% of *Shp2* expression in the $Shp2^{K14ce\text{-}cko}$ was likely attributed to the contamination of nonepithelial tissue; nevertheless, both *ΔNp63* and *Ngf* mRNAs were reduced dramatically in $Shp2^{K14ce\text{-}cko}$ as compared with those in $Shp2^{WT}$ controls. $*P < 0.05$ $(n = 4)$

reepihtelialization was evaluated every 6 h. We found that wound healing process in $Shp2^{K14ce\text{-}cko}$ adult mice was significantly hindered as compared with contol mice. Figure 9a shows that wound area was healed at 36–42 h post wound in control mice, while the mutant corneas still have uncovered defects even at 48 h after wound (Fig. 10a, b). H&E staining shows that 4–5 epithelial cell layers formed in the control mice at 48 h post wound, while there were no corneal epithelial cells covered in the $Shp2^{K14ce\text{-}cko}$ mice (Fig. 10c). These data are consistent with the notion that indeed cornea denervation and thinner epithelium delayed wound healing in $Shp2^{K14ce\text{-}cko}$ mouse.

Discussion

In current study, we, for the first time, demonstrate that *Shp2* ablation in corneal basal epithelial cells of adult mice resulted in thinner epithelium, nerve denervation, reduction of nerve sensation, and retardation of corneal

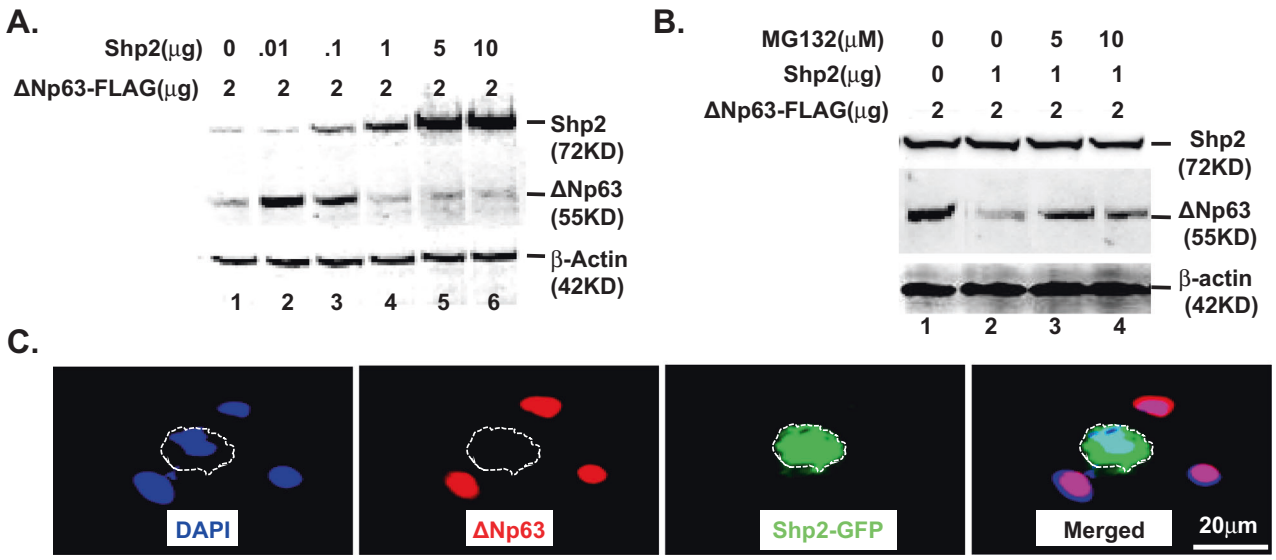

Fig. 9 Shp2 tightly regulated ΔNp63 protein level in HEK293 and HTCE cells. **a** Western blot analysis shows that Shp2 controls ΔNp63 protein level in a dosage dependent manner in HEK293 cells. Transfection of low dosages of *Shp2* plasmid DNA (0.01–0.1 g) increased ΔNp63 protein level. However, higher dosage of *Shp2* (≥1 g) decreased ΔNp63 protein level (**b**). MG132, a proteasome inhibitor, attenuated the inhibitory effect of high dosage of *Shp2* to ΔNp63 protein level. **c** Immunofluorescent staining shows that Shp2 (red) and ΔNp63 (green) were exclusively expressed in HTCE cotransfected with *CMV-Shp2-EGFP* and *CMV-ΔNp63* plasmid. All experiments were repeated three times and shows very similar results

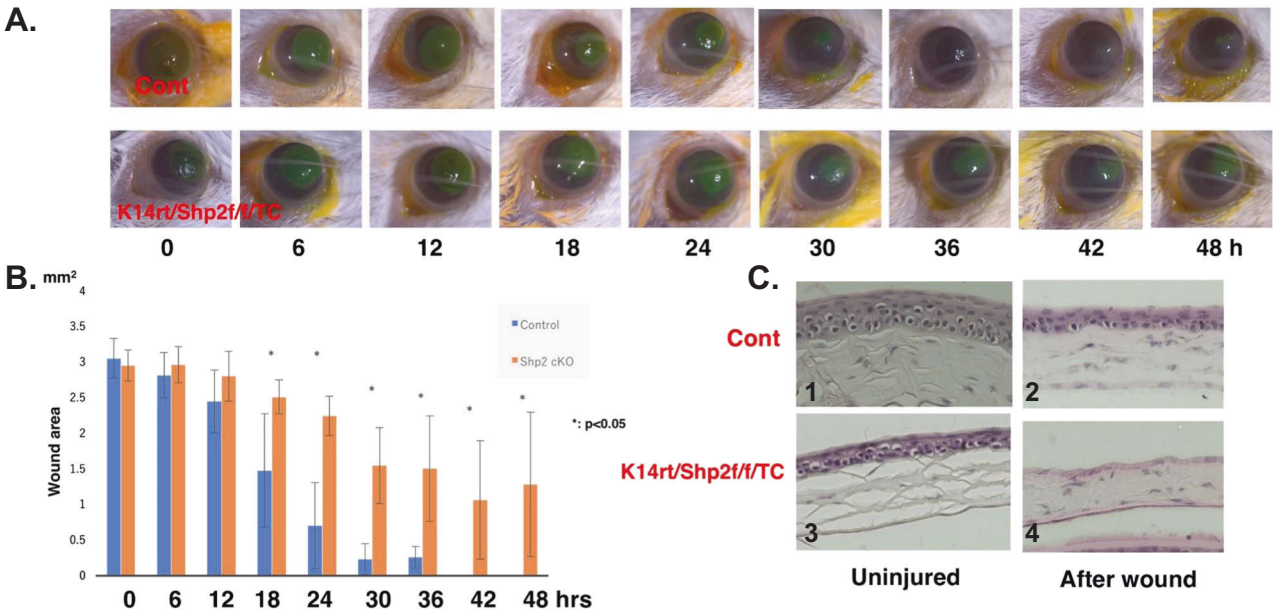

Fig. 10 Wound healing is delayed in $Shp2^{K14ce\text{-}cko}$ mice. **a** Photographs of corneal debridement healing process taken at different time points from 0 to 48 h post wound. *Shp2* deficiency in corneal basal epithelial cells (lower panel of **a**) impaired corneal wound healing process as compared with control mice (upper panel of **a**). **b** Bar chart of the size of remaining epithelial defects in the corneal epithelium at each time point. **c** H&E staining shows that there was no corneal epithelial cell layer covered in the $Shp2^{K14ce\text{-}cko}$ mice (C4), while 4–5 epithelial cell layers formed in the control mice (C2) at 48 h post wound. *($n = 6$, $P < 0.05$); NS no significance

debridement wound healing in the $Shp2^{K14ce\text{-}cko}$ mice. These defects resemble the clinical characteristics of NK in human. Furthermore, coculture experiments indicate that either knockdown of *Shp2*, *Mek*1/2, or *ΔNp63* in corneal epithelial cells encumbered neurite outgrowth of mouse primary trigeminal ganglia in vitro. At the molecular level, we found that Shp2 tightly regulated the ΔNp63 protein level probably through MEK–ERK signaling pathway in corneal epithelial cells. Therefore, Shp2 expression in corneal basal epithelial cells is of paramount importance in maintaining corneal homeostasis and innervation.

To study the pathophysiologic mechanism and the interaction between CE and trigeminal nerves in vivo of NK, some experimental animal models were produced by trigeminal denervation and investigated the consequence of cornea [41, 42]. Recently, we developed a new NK mouse model by coagulating the first branch of the trigeminal nerve [36]. Therefore, most of these works were focused on the effect of impaired trigeminal nerves to the development and homeostasis of CE. On the other hand, it is believed that close relationships exist between corneal epithelial cells and nerve fibers during corneal development and homeostasis [9, 23, 43]. For instance, corneal epithelial cells and sensory nerves work together to form specialized synapse-like structures in corneas [7]. Corneal epithelial cells function as surrogate Schwann cells for their sensory nerves [11]. However, not much attention has been paid to how corneal epithelial cells affect nerve innervation. There was no available animal model generated by specifically attacking the corneal cells and exploring the response of corneal nerves. The mouse strain, *K14rtTA*;*TC*;*Shp2*$^{flox/flox}$ used in current study might be the first transgenic animal model to fill this gap. In this model, *Shp2* gene is conditionally knocked out specifically in basal epithelial cells (K14 expressing cells) by Dox induction. Consequently, the homeostasis of CE was disrupted after Shp2 deletion, leading to thinner epithelium in the adult mutant mice (Fig. 1b–h). Notably, the phenotype of corneal epithelial thinning was followed by corneal denervation and reduction of corneal sensation (compare Fig. 1b–h with 1j). These data implied that sustaining the intact corneal epithelial stratification and integrity were crucial for preservation of corneal innervation and sensation. So this mouse strain could serve as a useful tool to study several critical questions such as what and how signals, signaling molecules, or neurotropic factors dreived from corneal epithelial cells triggering and/or involing in the pathogenesis of NK syndrome.

Taking advantage of our triple transgenic mouse strain, *K14rtTA*;*TC*;*Shp2*$^{flox/flox}$ and coculture in vitro experiments, we concluded that the signals from activated tyrosine protein kinase receptor (for example, phosphor-EGFR) mediated by Shp2–MEK–ERK–ΔNp63 signaling axis in corneal K14-expressing cells were critical both for the CE maintenance and innervation in adult mice. It has been well documented that ΔNp63 expressed in basal epithelial cells played essential roles in epithelial stratification and homeostasis in corneas and skins via multiple mechanisms such as promoting cell cycles and cell division direction [44–47]. Our study argues that ΔNp63 play an important role in basal cells for corneal epithelial innervation. The exact mechanism by which ΔNp63 regulated corneal innervation was not clear. The results of RNAi of *ΔNp63* reduced Ngf synthesis in TKE2 cells (Fig. 8a) and the downregulation of *ΔNp63* and *Ngf* expression in the cornea of *Shp2*$^{K14ce\text{-}cko}$ mice (Fig. 8b) suggest that soluble factor(s) such as Ngf may be associated with the corneal denervation in vivo and impairment of neurite outgrowth in coculture sysem. We also have performed preliminary RNAseq analysis and found that the expression of nerve growth factor (*NGF*), brain-derived neurotrophic factor (*BDNF*), and semaphorin (*Sema*) 6B, 4D, and 6D was significantly downregulated in *Shp2* siRNA or *ΔNp63* siRNA-treated TKE2 cells, while the expression of *Sema* 3D, 5A, 7A was increased (unpublished data). The role of these neurotrophic factors invovled in nerve growth, maintenance, proliferation, and survival [3, 48–51] required further investigation in the future.

One of the most interesting observations in this study was that Shp2 might strictly monitor the protein level of ΔNp63 in epithelial basal cells. Under naïve situation, Shp2 upregulated ΔNp63 expression (Fig. 9a, c). This is consistent with several previous reports, in which signals from EGFR-induced ΔNp63 expression in multiple cell lines [52]. More interestingly, in present study, we found that higher expression of Shp2 downregulated ΔNp63 protein level probably through proteasome-mediated degradation (Fig. 9b). This result was in agreement with our in vivo data, in which overexpression of *Shp2*^{E76K} [53] in corneal basal epithelial cells also led to corneal epithelial defects in *K14rtTA;tetO-Shp2*^{E76K} adult mice administered with Dox chow (our unpublished data). Since ΔNp63 protein stability is mainly regulated by ubiquitin-dependent proteasomal degradation pathway [54, 55], it is likely that fine-tuning of ΔNp63 protein level in corneal basal cells is critical to the epithelial cell stratification, maintenance, and nerve innervation during development and homeostasis of cornea.

Acknowledgements Supported in part by grants from NIH/NEI EY29071 (CYL); Ministry of Science and Technology (MOST) grant (Taiwan) 1042314B182A097MY3 (LKY); and Chang Gung Medical Research Project grants: CMRPG3E1522 (LKY); CMRPG3H1381 (LKY). We thank Hui-Chun Kung and Ya-Ling Chen for preparation of TEM studies at the Microscope Center of Chang-Gung Memorial Hospital, Linko, Taiwan.

Compliance with ethical standards

Conflict of interest The authors declare that they have no conflict of interest.

Publisher's note Springer Nature remains neutral with regard to jurisdictional claims in published maps and institutional affiliations.

References

1. Hassell JR, Birk DE. The molecular basis of corneal transparency. Exp Eye Res. 2010;91:326–35.
2. Müller LJ, Marfurt CF, Kruse F, Tervo TMT. Corneal nerves: structure, contents and function. Exp Eye Res. 2003;76:521–42.

3. Kubilus JK, Linsenmayer TF. Developmental guidance of embryonic corneal innervation: roles of Semaphorin3A and Slit2. Dev Biol. 2010;344:172–84.
4. Müller LJ, Vrensen GF, Pels L, Cardozo BN, Willekens B. Architecture of human corneal nerves. Investig Ophthalmol Vis Sci. 1997;38:985–94.
5. Shaheen BS, Bakir M, Jain S. Corneal nerves in health and disease. Surv Ophthalmol. 2014;59:263–85.
6. Mckenna CC, Lwigale PY. Innervation of the mouse cornea during development. Investig Ophthalmol Vis Sci. 2011;52:30–5.
7. Kubilus JK, Linsenmayer TF. Developmental corneal innervation: Interactions between nerves and specialized apical corneal epithelial cells. Investig. Ophthalmol Vis Sci. 2010;51:782–89.
8. Marfurt CF, Kingsley RE, Echtenkamp SE. Sensory and sympathetic innervation of the mammalian cornea. A retrograde tracing study. Investig Ophthalmol Vis Sci. 1989;30:461–72.
9. Lwigale PY. Embryonic origin of avian corneal sensory nerves. Dev Biol. 2001;239:323–37.
10. Müller LJ, Pels L, Vrensen GF. Ultrastructural organization of human corneal nerves. Investig Ophthalmol Vis Sci. 1996;37:476–88.
11. Stepp MA, Tadvalkar G, Hakh R, Pal-Ghosh S. Corneal Epithelial cells function as surrogate schwann cells for their sensory nerves. Glia. 2017;65:851–63.
12. Baker KS, Anderson SC, Romanowski EG, Thoft RA, SundarRaj N. Trigeminal ganglion neurons affect corneal epithelial phenotype. Influence on type VII collagen expression in vitro. Investig Ophthalmol Vis Sci. 1993;34:137–44.
13. Garcia-Hirschfeld J, Lopez-Briones LG, Belmonte C. Neurotrophic influences on corneal epithelial cells. Exp Eye Res. 1994;59:597–605.
14. Reid TW, Murphy CJ, Iwahashi CK, Foster BA, Mannis MJ. Stimulation of epithelial cell growth by the neuropeptide substance P. J Cell Biochem. 1993;52:476–85.
15. Chan KY, Haschke RH. Isolation and culture of corneal cells and their interactions with dissociated trigeminal neurons. Exp Eye Res. 1982;35:137–56.
16. Chan KY, Jones RR, Bark DH, Swift J, Parker JA Jr, Haschke RH. Release of neuronotrophic factor from rabbit corneal epithelium during wound healing and nerve regeneration. Exp Eye Res. 1987;45:633–46.
17. Oswald DJ, Lee A, Trinidad M, Chi C, Ren R, Rich CB, et al. Communication between corneal epithelial cells and trigeminal neurons is facilitated by purinergic (P2) and glutamatergic receptors. PLoS ONE. 2012;7:e44574.
18. Canner JP, Linsenmayer TF, Kubilus JK. Developmental regulation of trigeminal TRPA1 by the cornea. Investig Ophthalmol Vis Sci. 2014;56:29–36.
19. Bonini S, Rama P, Olzi D, Lambiase A. Neurotrophic keratitis. Eye. 2003;17:989–95.
20. Davis EA, Dohlman CH. Neurotrophic keratitis. Int Ophthalmol Clin. 2001;41:1–11.
21. Mastropasqua L, Massaro-Giordano G, Nubile M, Sacchetti M. Understanding the pathogenesis of neurotrophic keratitis: the role of corneal nerves. J Cell Physiol. 2017;232:717–24.
22. Sacchetti M, Lambiase A. Diagnosis and management of neurotrophic keratitis. Clin Ophthalmol. 2014;8:571–9.
23. Versura P, Giannaccare G, Pellegrini M, Sebastiani S, Campos EC. Neurotrophic keratitis: current challenges and future prospects. Eye Brain. 2018;10:37–45.
24. Ng GY, Yeh LK, Zhang Y, Liu H, Feng GS, Kao WW, et al. Role of SH2- containing tyrosine phosphatase Shp2 in mouse corneal epithelial stratification. Investig Ophthalmol Vis Sci. 2013;54:7933–42.
25. Freeman RM Jr, Plutzky J, Neel BG. Identification of a human src homology 2- containing protein-tyrosine-phosphatase: a putative homolog of Drosophila corkscrew. Proc Natl Acad Sci USA. 1992;89:11239–43.
26. Jamieson CR, van der Burgt, Brady AF, van Reen M, Elsawi MM, Hol F, et al. Mapping a gene for Noonan syndrome to the long arm of chromosome 12. Nat Genet. 1994;8:357–60.
27. Chan RJ, Feng GS. PTPN11 is the first identified proto-oncogene that encodes a tyrosine phosphatase. Blood. 2007;109:862–67.
28. Dance M, Montagner A, Salles JP, Yart A, Raynal P. The molecular functions of Shp2 in the Ras/Mitogen-activated protein kinase (ERK1/2) pathway. Cell Signal. 2008;20:453–9.
29. Matozaki T, Murata Y, Saito Y, Okazawa H, Ohnishi H. Protein tyrosine phosphatase SHP-2: a proto-oncogene product that promotes Ras activation. Cancer Sci. 2009;100:1786–93.
30. Grossmann KS, Rosário M, Birchmeier C, Birchmeier W. The tyrosine phosphatase Shp2 in development and cancer. Adv Cancer Res. 2010;106:53–89.
31. Nguyen H, Rendl M, Fuchs E. Tcf3 governs stem cell features and represses cell fate determination in skin. Cell. 2006;127:171–83.
32. Perl AK, Wert SE, Nagy A, Lobe CG, Whitsett JA. Early restriction of peripheral and proximal cell lineages during formation of the lung. Proc Natl Acad Sci USA. 2002;99:10482–7.
33. Feng G, Mellor RH, Bernstein M, Keller-Peck C, Nguyen QT, Wallace M, et al. Imaging neuronal subsets in transgenic mice expressing multiple spectral variants of GFP. Neuron. 2000;28:41–51.
34. Zhang EE, Chapeau E, Hagihara K, Feng GS. Neuronal Shp2 tyrosine phosphatase controls energy balance and metabolism. Proc Natl Acad Sci USA. 2004;101:16064–69.
35. Aykut V, Elbay A, Uçar Çigdem, Esen F, Durmus A, Karadag R, et al. Corneal sensitivity and subjective complaints of ocular pain in patients with fibromyalgia. Eye. 2018;32:763–67.
36. Okada Y, Sumioka T, Ichikawa K, Sano H, Nambu A, Kobayashi K, et al. Sensory nerve supports epithelial stem cell function in healing of corneal epithelium in mice: the role of trigeminal nerve transient receptor potential vanilloid 4. Lab Investig. 2019;99:210–30.
37. Kubota M, Shimmura S, Miyashita H, Kawashima M, Kawakita T, Tsubota K, et al. The anti-oxidative role of ABCG2 in corneal epithelial cells. Investig Opthalmol Vis Sci. 2010;51:5617–22.
38. Vandewauw I, Owsianik G, Voets T. Systematic and quantitative mRNA expression analysis of TRP channel genes at the single trigeminal and dorsal root ganglion level in mouse. BMC Neurosci. 2013;14:21.
39. Suzuki M, Mizuno A, Kodaira K, Imai M. Impaired pressure sensation in mice lacking TRPV4. J Biol Chem. 2003;278:22664–68.
40. Aceto N, Sausgruber N, Brinkhaus H, Gaidatzis D, Martiny-Baron G, Mazzarol G, et al. Tyrosine phosphatase SHP2 promotes breast cancer progression and maintains tumor-initiating cells via activation of key transcription factors and a positive feedback signaling loop. Nat Med. 2012;18:529–37.
41. Ferrari G1, Chauhan SK, Ueno H, Nallasamy N, Gandolfi S, Borges L, et al. A novel mouse model for neurotrophic keratopathy: trigeminal nerve stereotactic electrolysis through the brain. Investig Opthalmol Vis Sci. 2011;52:2532–9.
42. Wong EK, Kinyamu RD, Graff JM, Chak G, Wong MN, Agnic H, et al. A rat model of radiofrequency ablation of trigeminal innervation via a ventral approach with stereotaxic surgery. Exp Eye Res. 2004;79:297–303.
43. He J, Bazan HE. Neuroanatomy and neurochemistry of mouse cornea. Investig Ophthalmol Vis Sci. 2016;57:664–74.
44. Koster MI, Roop DR. Mechanisms regulating epithelial stratification. Annu Rev Cell Dev Biol. 2007;23:93–113.
45. Shalom-Feuerstein R, Lena AM, Zhou H, De La Forest Divonne S, Van Bokhoven H, Candi E, et al. ΔNp63 is an ectodermal

gatekeeper of epidermal morphogenesis. Cell Death Differ. 2011; 18:887–96.
46. Zhang Y, Yeh LK, Zhang S, Call M, Yuan Y, Yasunaga M, et al. Wnt/β-catenin signaling modulates corneal epithelium stratification via inhibition of Bmp4 during mouse development. Development. 2015;142:3383–93.
47. Zhang Y, Call MK, Yeh LK, Liu H, Kochel T, Wang IJ, et al. Aberrant expression of a β-catenin gain-of-function mutant induces hyperplastic transformation in the mouse cornea. J Cell Sci. 2010;123:1285–94.
48. Barbieri CE, Tang LJ, Brown KA, Pietenpol JA. Loss of p63 leads to increased cell migration and up-regulation of genes involved in invasion and metastasis. Cancer Res. 2006;66:7589–97.
49. Kobayashi T, Shiraishi A, Hara Y, Kadota Y, Yang L, Inoue T, et al. Stromal- epithelial interaction study: the effect of corneal epithelial cells on growth factor expression in stromal cells using organotypic culture model. Exp Eye Res. 2015;135:109–17.
50. Uren RT, Turnley AM. Regulation of neurotrophin receptor (Trk) signaling: suppressor of cytokine signaling 2 (SOCS2) is a new player. Front Mol Neurosci. 2014;7:39.
51. Koncina E, Roth L, Gonthier B, Bagnard D. Axon growth and guidance, Volume 621, New York: Springer; 2007. p. 50–64.
52. Chu WK, Lee KC, Chow SE, Chen JK. Dual regulation of the ΔNp63 transcriptional activity by ΔNp63 in human nasopharyngeal carcinoma cell. Biochem Biophys Res Commun. 2006;342:1356–60.
53. Schneeberger VE, Luetteke N, Ren Y, Berns H, Chen L, Foroutan P, et al. SHP2E76K mutant promotes lung tumorigenesis in transgenic mice. Carcinogenesis. 2014;35:1717–25.
54. Li C, Xiao ZX. Regulation of p63 protein stability via ubiquitin-proteasome pathway. Biomed Res. Int. 2014;2014:175721.
55. Armstrong SR, Wu H, Wang B, Abuetabh Y, Sergi C, Leng RP. The regulation of tumor suppressor p63 by the ubiquitin-proteasome system. Int J Mol Sci. 2016;17:E2041.